ALLEN INSTITUTE for BRAIN SCIENCE

Allen Brain Observatory

TECHNICAL WHITEPAPER:
STIMULUS SET AND RESPONSE ANALYSIS

INTRODUCTION

The Visual Coding data set of the Allen Brain Observatory characterizes single cells and populations of cells by the responses of neurons in the mouse visual cortex to a range of visual stimuli. Neurons throughout the visual system have typically been characterized by their *receptive field* (Hubel and Wiesel, 1962; Kuffler, 1953). The receptive field is a property of a neuron computed from measured responses that summarizes the features of the visual stimuli that drive that cell's activity. In its simplest form, a cell's receptive field is the region in visual space where a visual stimulus will elicit a response from the cell. The earliest cells in the visual pathway respond to spots of light or dark, and thus are described by circular spatial receptive fields. An early and famous finding in visual neuroscience is that there are neurons in the visual cortex that respond to oriented bars of light or dark against dark or bright backgrounds, respectively, rather than spots (Hubel and Wiesel, 1962). Further, there are even cells that respond to the movement of bars of light or dark, showing selectivity for motion in specific directions. These responses indicate that more sophisticated spatial and temporal structure is required to describe the receptive fields of these cells. A general observation from mammalian vision is that higher visual areas tend to respond to more complex aspects of the visual field relative to lower areas. These differences indicate that the different neurons and visual areas have distinct functional properties (Andermann et al., 2011; Marshel et al., 2011). By exploring the relationship between the spatial and temporal response characteristics of visual neurons, the Allen Brain Observatory aims to characterize these properties throughout the mouse visual cortex, and explore the progressive coding of visual information in this pathway.

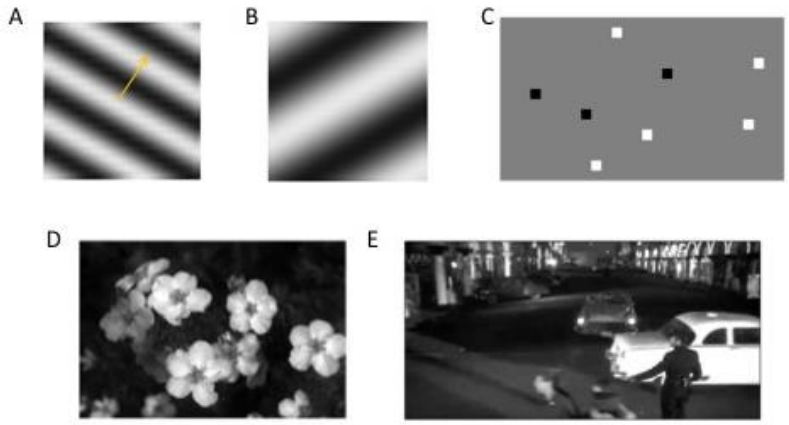

Figure 1. Stimulus set for the Allen Brain Observatory – Visual Coding. A) Drifting gratings B) Static gratings C) Locally sparse noise D) Natural scenes E) Natural movies.

The spatial and temporal receptive field of neurons in the visual cortex can be parameterized efficiently and systematically using *synthetic* stimuli, including *sinusoidal gratings* (both drifting and static) and *locally sparse noise* (**Fig. 1A-C**). The grating stimulus is a simple pattern whose intensity varies periodically along one dimension, and is constant in the other dimension. The grating can vary in its spatial frequency (the period of

the grating), temporal frequency (the speed at which the grating moves), and orientation (the angle of the grating). By systematically surveying these parameters, we can characterize the temporal and spatial response profiles, allowing us to, for example, identify a cell's preferred orientation as well as its preferred spatial and temporal frequencies. The cells' receptive fields can be further measured using the locally sparse noise stimulus. This stimulus flashes white or black spots in different parts of visual space. By characterizing the responses to these spots across the visual field, the spatial size and shape of the receptive field can be mapped, and we do so separately for both white ("On") and dark ("Off") stimuli. Collectively, these response characteristics can be used to build an initial map of functional properties throughout the cortical circuit.

Receptive fields measured using *synthetic* stimuli, such as gratings and noise, often produce models that fail to predict responses to *natural* stimuli (David et al., 2004). This is, in part, because natural stimuli are more complex, and contain strong correlations in both time and space that are absent from the simple synthetic stimuli. In order to explore neural response to natural stimuli, we employ both flashed natural scenes and several natural movie clips (**Fig. 1D, E**). These stimuli allow us to measure cell's responses to natural scenes and to explore non-linear processing in their receptive fields.

This set of responses to these synthetic and natural stimuli provides us with a way of characterizing the activity of cells across the mouse visual cortex and feeds into both our efforts and the efforts of the field to build models of the visual system and of neural computation.

VISUAL STIMULUS HARDWARE

Visual stimuli were generated using custom scripts written in PsychoPy (Peirce, 2007, 2008) and were displayed using an ASUS PA248Q LCD monitor, with 1920x1200 pixels. The monitor was positioned 15 cm from the mouse's eye, and spanned 120° x 95° of visual space without accounting for stimulus warping.

Each monitor was gamma corrected using a USB-650 Red Tide Spectrometer (Ocean Optics). Luminance was measured using a SpectroCAL MKII Spectroradiometer (Cambridge Research Systems). Monitors were used at a Brightness setting of 30% and Contrast at 50%, corresponding to a mean luminance of 50 cd/m2 (**Fig. 2**).

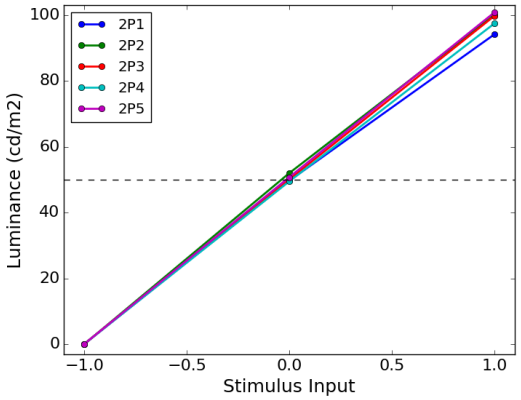

Figure 2. Luminance values for the monitors used on each imaging system. Stimulus input -1 is black, 0 is mean gray, 1 is white.

VISUAL STIMULUS WARPING

To account for the close viewing angle of the mouse, a spherical warping was applied to all stimuli to ensure that the apparent size, speed, and spatial frequency were constant across the monitor as seen from the mouse's perspective (**Fig. 3**). Several pixels in the stimulus template in the NWB files do not get displayed on the monitor following this warping, particularly in the corners of the images and movies. The Software Development Kit (AllenSDK) contains functions for implementing this mask as well as for masking the stimulus template to indicate which pixels are on the monitor (make_display_mask).

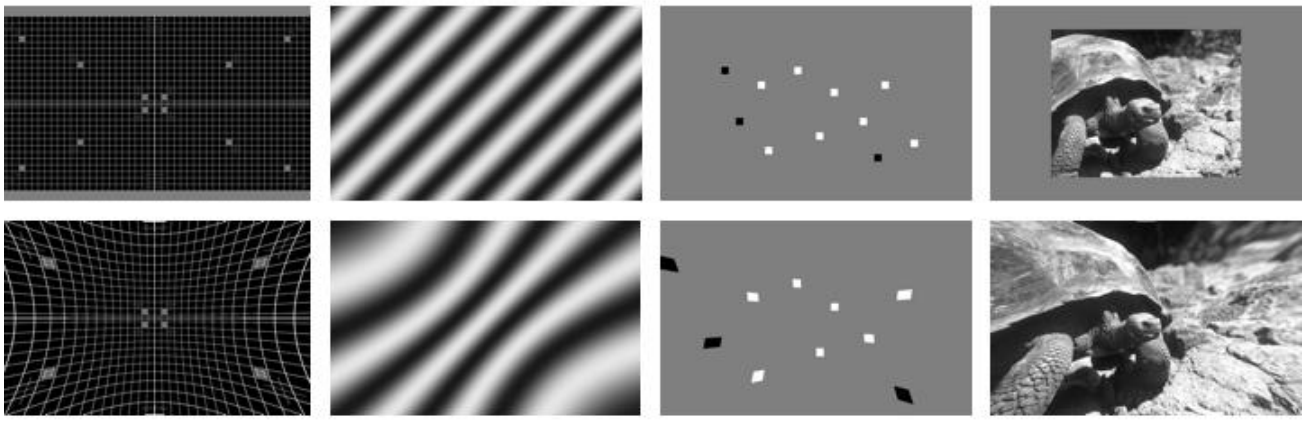

Figure 3. Demonstration of stimulus warping. Top, unwarped images. Bottom, warped images.

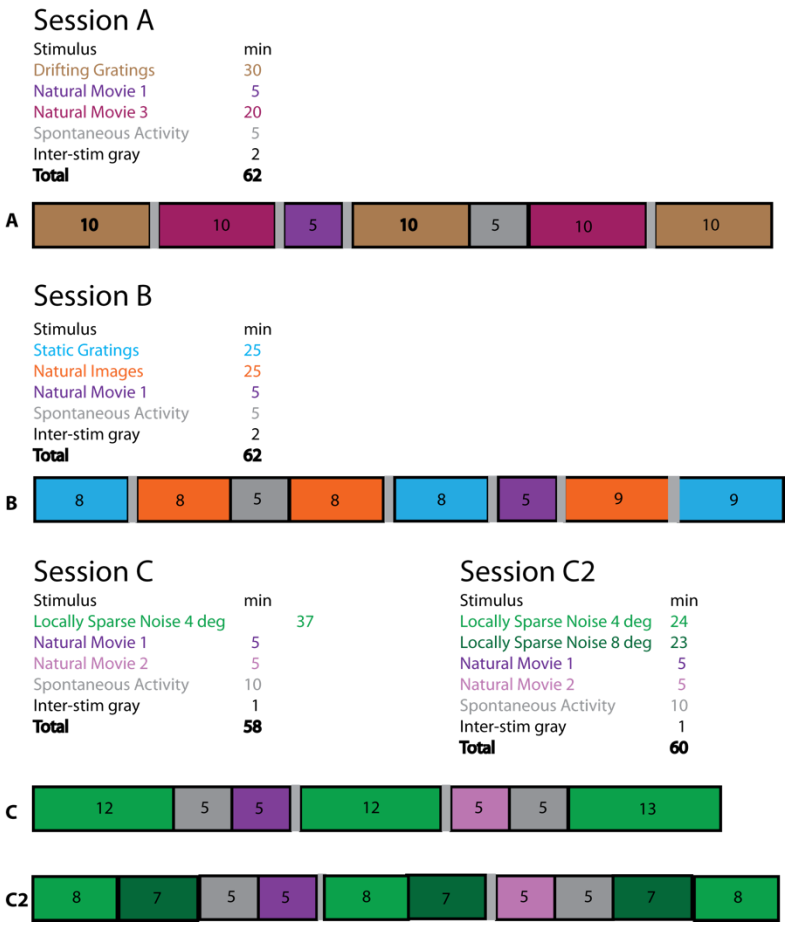

Figure 4. Sequence of visual stimuli across three sessions.

VISUAL STIMULUS DEFINITION

To characterize the visual responses of neurons in the mouse visual cortex, a battery of stimuli were used that included drifting gratings, static gratings, locally sparse noise, natural scenes and natural movies (**Fig. 1**). In addition, imaging was performed during epochs of spontaneous activity, and running speed and eye movement were measured throughout all imaging.

To characterize responses to the entire visual stimulus set described here, the visual stimuli were distributed across three imaging sessions (**Fig. 4**). Each session contained a combination of stimuli that were broken into segments of 5-13 minutes and interleaved with each other. Additionally, each session contained at least one 5-minute epoch of spontaneous activity and a complete presentation of the Natural Movie 1 stimulus. Data released in the June 2016 and October 2016 releases were collected using sessions A, B and C. Data released in the June 2017 release were collected using sessions A, B and C2.

Drifting Gratings

Stimulus. This stimulus was used to measure the direction tuning, orientation tuning and temporal frequency tuning of the cells. The total stimulus duration was 31.5 minutes.

The stimulus consisted of a full field drifting sinusoidal grating at a single spatial frequency (0.04 cycles/degree) and contrast (80%). The grating was presented at 8 different directions (separated by 45°) and at 5 temporal frequencies (1, 2, 4, 8, 15 Hz). Each grating was presented for 2 seconds, followed by 1 second of mean luminance gray before the next grating. Each grating condition (direction & temporal frequency combination) was presented 15 times, in a random order. There were blank sweeps (i.e. mean luminance gray instead of grating) presented approximately once every 20 gratings.

Analysis. For each trial, the ΔF/F for each cell was calculated using the mean fluorescence of the preceding 1 second as the baseline F_o (**Fig. 5A**).

$$\frac{\Delta F}{F} = \frac{F - F_o}{F_o}$$

The evoked response was defined as the mean ΔF/F during the grating presentation (**Fig. 5B**). Each condition was presented 15 times, and responses to all presentations were averaged together. The preferred direction and temporal frequency condition was defined as that grating condition that evoked the largest mean response.

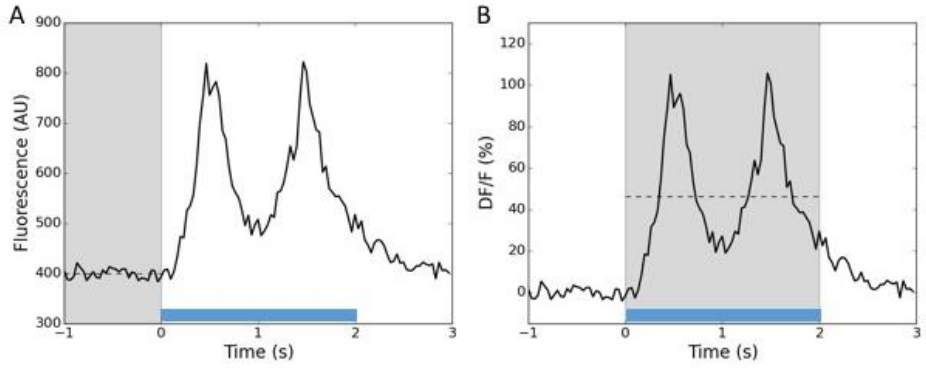

Figure 5. Calculating the response to each stimulus presentation. A) Raw fluorescence of a cell aligned to the presentation of a drifting grating stimulus (from time 0-2s). The mean fluorescence during the preceding 1 s (shaded gray, dashed line represents the mean) is used as the baseline F_o to compute ΔF/F. **B**) ΔF/F during presentation of drifting grating. The mean ΔF/F during the grating presentation (shaded gray, dashed line represents the mean) defines the evoked response of this cell to this grating. Grating presentation occurs during the time indicated by the blue bar.

*Metrics (see **Table 1**).* The orientation selectivity index (OSI) was computed as

$$OSI = \frac{R_{pref} - R_{orth}}{R_{pref} + R_{orth}}$$

where R_{pref} is the mean response to the preferred orientation at the preferred temporal frequency and R_{orth} is the mean response to the orthogonal directions.

The Orientation and Direction Selectivity Indices (OSI and DSI) are computed using a locally-measured DF/F. As DF/F values can be negative, especially for non-preferred stimulus conditions, some OSI and DSI values can be greater than 1. We chose to filter out OSI and DSI values below 0 or above 2, chosen by inspecting the distribution of OSI values for the drifting gratings stimulus as released in June 2016 (**Fig. 6**, **Table 2**).

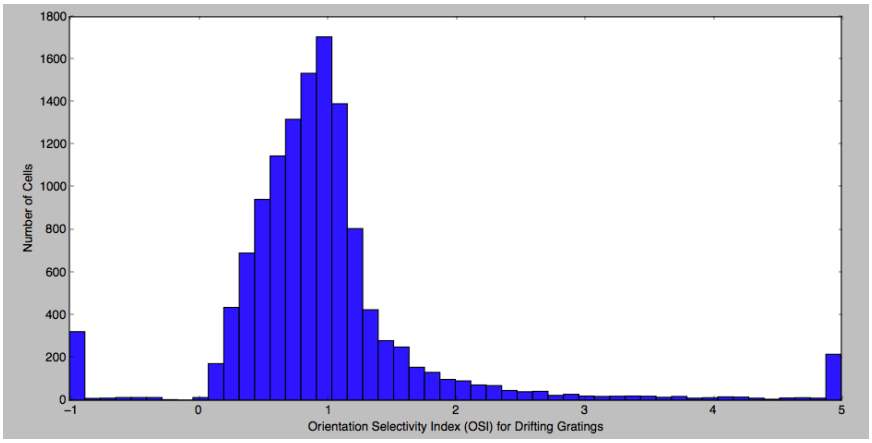

Figure 6. Distribution of OSI values for all cells prior to filtering.

Orientation tuning was also measured using the global orientation selectivity index (gOSI) (Ringach et al., 1997) defined as:

$$gOSI = \frac{\sum R_\theta e^{2i\theta}}{\sum R_\theta}$$

where R_θ is the mean response to grating at direction θ at the preferred temporal frequency.

Direction selectivity index (DSI) was computed as

$$DSI = \frac{R_{pref} - R_{null}}{R_{pref} + R_{null}}$$

where R_{null} is the mean response to the opposite direction at the preferred temporal frequency.

Direction tuning was also measure using the global direction selectivity index (gDSI), defined as:

$$gDSI = \frac{\sum R_\theta e^{i\theta}}{\sum R_\theta}$$

The temporal frequency discriminability index was computed as:

$$TFDI = \frac{R_{max} - R_{min}}{R_{max} - R_{min} + 2\sqrt{SSE/(N-M)}}$$

where R_{max} is the response at the preferred direction and temporal frequency, R_{min} is the response at the temporal frequency that elicits the smallest response at the preferred direction, SSE is the sum of squared errors of all responses at the preferred direction, N is the number of trials, and M is the number of temporal frequencies (DeAngelis and Uka, 2003).

The response reliability was calculated as the mean trial-to-trial correlation:

$$reliability = \frac{2}{T^2 - T}\sum_{i=1}^{T}\sum_{j=i+1}^{T}\rho(f_i, f_j)$$

where f_i is the ΔF/F response of the i-th trial of a cell's preferred condition and T is the number of trials at the preferred condition (Rikhye and Sur, 2015).

To determine if a cell was significantly responsive to the drifting grating stimulus, a one-way ANOVA was computed comparing the evoked responses to all of the 40 drifting grating stimulus conditions (8 directions x 5 temporal frequencies) as well as the blank sweep. A cell with a p-value less than 0.05 was considered to be responsive to this stimulus.

The mean running speed of the mouse was computed for each grating presentation. To calculate the running modulation, the presentations of the preferred grating condition (peak direction and temporal frequency) were broken into "stationary" trials (those when the speed was less than 1 cm/s) and "running" trials (those when the speed was greater than 1 cm/s). Provided that there were at least 10% of trials in each condition, the running modulation was defined as:

$$run_{mod} = C \times \frac{R_{max} - R_{min}}{|R_{min}|}$$

where R_{max} is the larger of the response when the mouse is running or when the mouse is stationary, and R_{min} is the smaller of the two. If R_{max} is the response when the mouse is running, C=1. If R_{max} is the response when the mouse is stationary, C=-1.

The p_run value reports the p-value of an independent T-test comparing the mean responses of the stationary trials to the mean responses of the running trials.

In order to compare the stimulus preferences of different neurons, we computed the signal correlation of each pair of neurons. The signal correlation of two neurons is the correlation coefficient between the trial-averaged response of those neurons to each stimulus condition, averaged across stimulus conditions. We computed the Spearman correlation of the responses because of the potential non-Gaussianity of the calcium responses. The SDK includes an option to compute the signal correlation using the Pearson correlation instead.

$$signal\ correlation_{i,j} = \frac{1}{N}\sum_{k=1}^{N}\rho(\langle f_{i,k}\rangle, \langle f_{j,k}\rangle)$$

Where N is the number of stimulus conditions, $\langle f_{i,k}\rangle$ is the mean ΔF/F response of cell *i* to stimulus condition *k*.

The representational similarity measures whether different stimuli recruit similar populations of neurons (Kriegeskorte et al., 2008). It is analogous to the signal correlation, but with the roles of the neurons and stimuli exchanged. The representational similarity of two stimuli was computed as the correlation between the trial-averaged responses to those two stimuli, averaged across neurons. We computed the Spearman correlation of the responses because of the potential non-Gaussianity of the calcium responses. The SDK includes an option to compute the representational similarity using the Pearson correlation instead.

The noise correlation measures the similarity of two neurons' response fluctuations. For each stimulus trial, we computed the correlation coefficient of two neurons' responses to that trial, and then averaged across all trials. We computed the Spearman correlation of the responses because of the potential non-Gaussianity of the calcium responses. The SDK includes an option to compute the representational similarity using the Pearson correlation instead.

$$noise\ correlation_{i,j} = \frac{1}{N}\sum_{k=1}^{N}\rho(f_{i,k}, f_{j,k})$$

Where $f_{i,k}$ is the ΔF/F response of cell *i* to trial k, and N is the number of trials (across all stimulus conditions).

Visualizations. Each cell's response to the drifting grating stimulus is represented on a "Star plot" (**Fig. 7A**), capturing the orientation and temporal frequency tuning as well as the trial-to-trial variability of responses to each stimulus condition. Each arm of the plot represents one of the directions of the grating while each ring represents the temporal frequency of the grating, with the lowest temporal frequency at the center and the highest temporal frequency on the outside. At each intersection are fifteen dots, each representing the cell's response to an individual trial of that stimulus condition. The intensity of each dot corresponds to the strength of the cell's response to that trial and the dots are organized with the strongest response in the center and weaker responses spiraling outward. The color scale ranges from white, which is the mean response to the blank sweep, to dark red, which is three standard deviations above the mean response to all stimulus conditions together.

For each cell, we plot a histogram of the signal correlation of that cell with all the other cells imaged in that experiment session, capturing the similarity of its tuning to the tuning of other cells (**Fig. 7B).**

The representational similarity matrix for each experiment is presented as a heatmap (**Fig. 7C**). Each row (and column) corresponds to a particular stimulus condition (e.g. direction and temporal frequency). The color of the element in the *i*th row and the *j*th column of the matrix indicates whether the mean response to stimulus *i* and *j* were positively correlated (red), negatively correlated (blue), or uncorrelated (white). The diagonal (*i*=*j*) was removed. The stimulus conditions are coded along the top and left edges of the matrix, with a legend at the bottom.

A comparison of signal and noise correlations for all cells in an experiment is plotted for each stimulus (**Fig. 7D**).

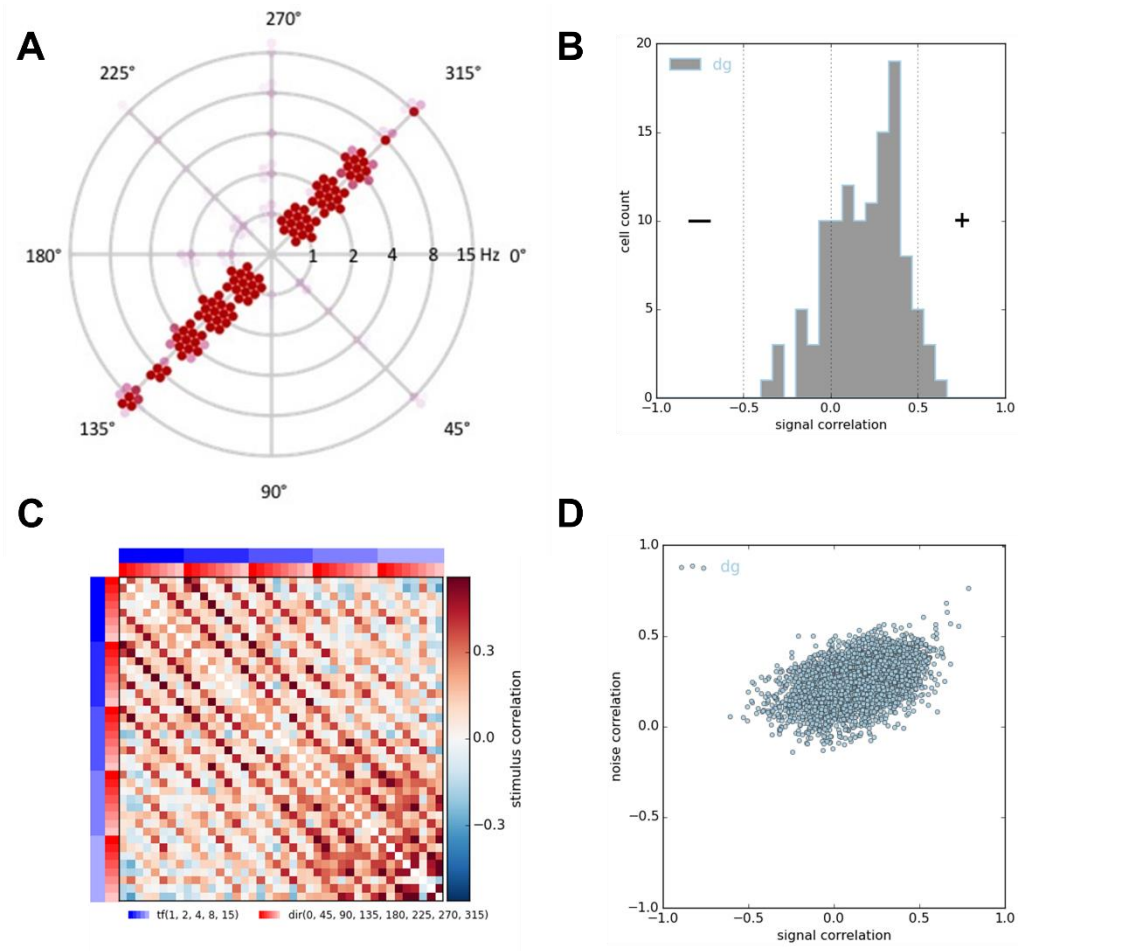

Figure 7. Visualizations of drifting grating responses. A, The star plot captures the response of a neuron to drifting gratings. **B,** Histogram of signal correlations of one cell with all other cells in the experiment, shown here for the responses to the drifting grating stimulus. **C,** Representational similarity matrix, shown here for responses to drifting gratings. **D**, Noise correlations vs. signal correlations.

Static Gratings

Stimulus. This stimulus was used to measure the spatial frequency tuning and the orientation tuning of the cells, providing a finer measurement of orientation than provided from the drifting grating stimulus. The total stimulus duration was 26 minutes.

The stimulus consisted of a full field static sinusoidal grating at a single contrast (80%). The grating was presented at 6 different orientations (separated by 30°), 5 spatial frequencies (0.02, 0.04, 0.08, 0.16, 0.32 cycles/degree), and 4 phases (0, 0.25, 0.5, 0.75). The grating was presented for 0.25 seconds, with no inter-grating gray period. Each grating condition (orientation, spatial frequency, and phase) was presented ~50 times in a random order. There were blank sweeps (i.e. mean luminance gray instead of grating) presented roughly once every 25 gratings.

Analysis. For each trial, the $\Delta F/F$ for each cell was calculated using the mean fluorescence of the preceding 1 second as the baseline F_0. As there is no inter-grating gray period, this 1 second window spans 4 different grating presentations. The evoked response to each grating was defined as the mean change in fluorescence during the 0.5 second period following the start of the grating presentation compared to the 1 second preceding the grating presentation (**Fig. 8**). This 0.5 second window was chosen to accommodate the kinetics of the GCaMP6f indicator. The window spans both the presentation of the specified grating and the following grating.

Each grating condition was presented ~50 times, and the responses to all presentations were averaged together. As the gratings are presented in random order, any effects of the different grating conditions preceding or following the specified grating should average out across the 50 trials. The preferred orientation, spatial frequency and phase conditions were identified as the grating condition that evoked the largest mean response.

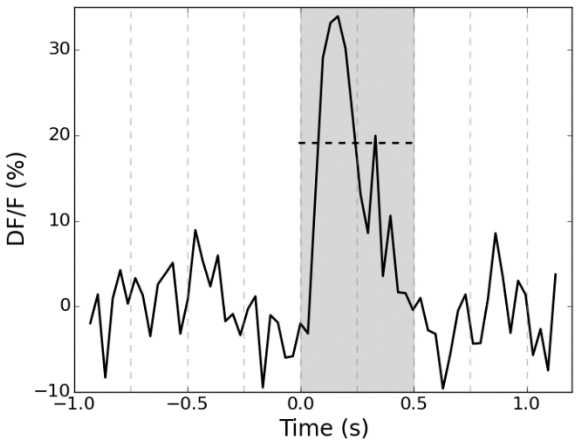

Figure 8. Calculating response to flashed stimuli. ΔF/F during presentation of a flashed stimulus (e.g. static grating). Stimulus transitions are indicated by the vertical dotted lines. For a specific stimulus trial, which starts at t=0, F_o is calculated as the mean fluorescence during the preceding 1 second. The mean ΔF/F during the gray shaded time defines the evoked response of this cell to this stimulus trial (dashed line represents the mean).

*Metrics (see **Table 1**).* The orientation selectivity index (OSI) was computed as:

$$OSI = \frac{R_{pref} - R_{orth}}{R_{pref} + R_{orth}}$$

where R_{pref} is the mean response to the preferred orientation at the preferred spatial frequency and phase and R_{orth} is the response to the orthogonal directions.

Orientation tuning was also measured using the global orientation selectivity index (gOSI) defined as:

$$gOSI = \frac{\sum R_\theta e^{2i\theta}}{\sum R_\theta}$$

where R_θ is the mean response to grating at direction θ at the preferred spatial frequency.

The spatial frequency discriminability index was computed as:

$$SFDI = \frac{R_{max} - R_{min}}{R_{max} - R_{min} + 2\sqrt{SSE/(N-M)}}$$

where R_{max} is the response at the preferred orientation and spatial frequency, R_{min} is the response at the spatial frequency that elicits the smallest response at the preferred orientation, SSE is the sum of squared errors of all responses at the preferred orientation , N is the number of trials, and M is the number of spatial frequencies (DeAngelis and Uka, 2003).

The response reliability was calculated as the mean trial-to-trial correlation:

$$reliability = \frac{2}{T^2 - T}\sum_{i=1}^{T}\sum_{j=i+1}^{T}\rho(f_i, f_j)$$

where f_i is the ΔF/F response of the i-th trial of a cell's preferred condition and T is the number of trials at the preferred condition (Rikhye and Sur, 2015).

To determine if a cell was significantly responsive to the static grating stimulus, a one-way ANOVA was computed comparing the responses to all of the 120 different grating conditions (6 orientation X 5 spatial frequencies X 4 phases). A cell with a p-value less than 0.05 was considered to be responsive to this stimulus.

For each trial of each grating, a one-way ANOVA was computed comparing the ΔF/F during the 1 second preceding the grating presentation with the ΔF/F during the 0.5 second response period. Any trial with a p-value less than 0.05 was considered a significant trial. For each cell, the response variability is the percent of trials that had a significant response at the preferred condition.

For the preferred stimulus condition, the time-to-peak was measured as the time of the peak of the mean response relative to the onset of the grating presentation.

The mean running speed of the mouse was computed for each grating presentation. To calculate the running modulation, the presentations of the preferred grating condition (preferred orientation, spatial frequency and phase) were broken into "stationary" trials (those when the speed was less than 1 cm/s) and "running" trials (those when the speed was greater than 1 cm/s). Provided that there were at least 10% of trials in each condition, the running modulation was defined as:

$$run_{mod} = C \times \frac{R_{max} - R_{min}}{|R_{min}|}$$

where R_{max} is the larger of the response when the mouse is running or when the mouse is stationary, and R_{min} is the smaller of the two. If R_{max} is the response when the mouse is running, C=1. If R_{max} is the response when the mouse is stationary, C=-1.

The p_run value reports the p-value of an independent T-test comparing the mean responses of the stationary trials to the mean responses of the running trials.

Visualization. Each cell's response to the static grating stimulus is represented in a "fan plot" (**Fig. 9A**), capturing the orientation and spatial frequency tuning as well as the trial-to-trial variability of the responses to each stimulus condition. Each arm of the plot represents one of the grating orientations while each arc represents a spatial frequency, with the lowest spatial frequency near the center and high frequencies radiating outward. At the intersections of these axes are four lobes, each corresponding to a different phase. Each lobe contains an array of dots, the color and intensity of which correspond to the strength of the response to each trial. The dots are organized with the strongest response in the center and weaker responses spiraling outward. The color scale of the dots ranges from white, which is the mean response to the blank sweep, to dark red, which is three standard deviations above the mean response to all stimulus conditions together.

For each cell, we plot a histogram of the signal correlation of that cell with the other cells imaged in that experiment session, capturing the similarity of its tuning to the tuning of other cells. As the static gratings and natural scenes were presented in the same imaging session, the signal correlations of cells to these stimuli were plotted together, allowing comparisons of whether pairs of cells had similar correlations to these different stimuli (**Fig. 9B**).

The representational similarity matrix for each experiment is presented as a heatmap. Each row (and column) corresponds to a particular stimulus condition (e.g. orientation, spatial frequency, and phase). The color of the element in the *i*th row and the *j*th column of the matrix indicates whether the mean response to stimulus *i* and *j* were positively correlated (red), negatively correlated (blue), or uncorrelated (white). The diagonal (*i=j*) was removed. The stimulus conditions are coded along the top and left edges of the matrix, with a legend at the bottom. (**Fig. 9C**).

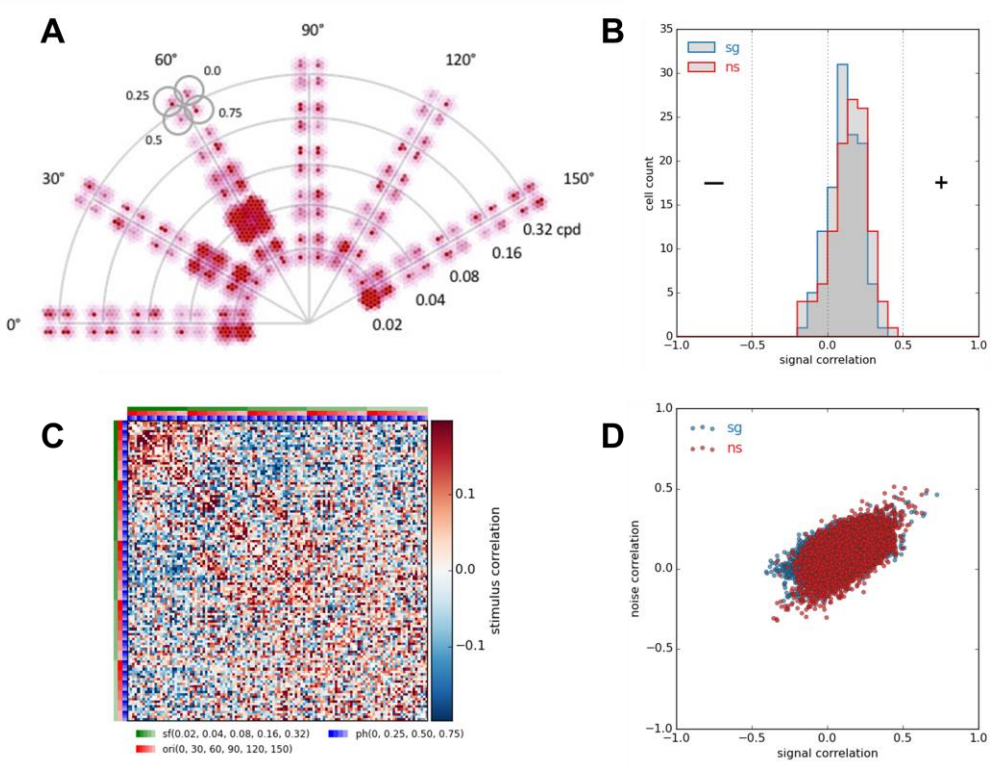

Figure 9. Visualizations of static grating responses. A, The fan plot captures the spatial frequency and orientation tuning of a cell. **B**, Histogram of signal correlations of one cell with all the other cells in the experiment, here for the responses to the static gratings and natural scenes stimuli. **C,** Representational similarity matric for static gratings. **D,** Noise correlations vs signal correlations, plotted for both static gratings and natural scenes.

We plot the comparison of signal and noise correlations for all cells in an experiment. As static gratings and natural scenes were presented in the same imaging session, these correlations are plotted in a single plot (**Fig. 9D**).

Locally Sparse Noise

Stimulus. This stimulus was used to measure the spatial receptive field, including both on and off subunits. The total stimulus duration was 37.5 minutes.

For data published in June 2016 and October 2016, data was collected using the Session C stimulus (**Fig. 4**). The Locally Sparse Noise stimulus consisted of a 16 x 28 array of pixels, each 4.65 degrees on a side. Please note, while this stimulus is called Locally Sparse Noise 4 deg, the pixel size is in fact 4.65 degrees. For each frame of the stimulus (which was presented for 0.25 seconds), a small number of pixels were white and a small number were black, while the rest were mean gray. The white and black spots were distributed such that no two spots were within 5 pixels of each other. Each time a given pixel was occupied by a black (or white) spot, there was a different array of other pixels occupied by either black or white spots. As a result, when all of the frames when that pixel was occupied by the black spot were averaged together, there was no significant structure surrounding the specified pixel (**Fig. 10**). Further, the stimulus was well balanced with regards to the contrast of the pixels, such that while there was a higher probability of a pixel being occupied just outside of the 5-pixel exclusion zone, the probability was equal for pixels of both contrast (**Fig. 11**).

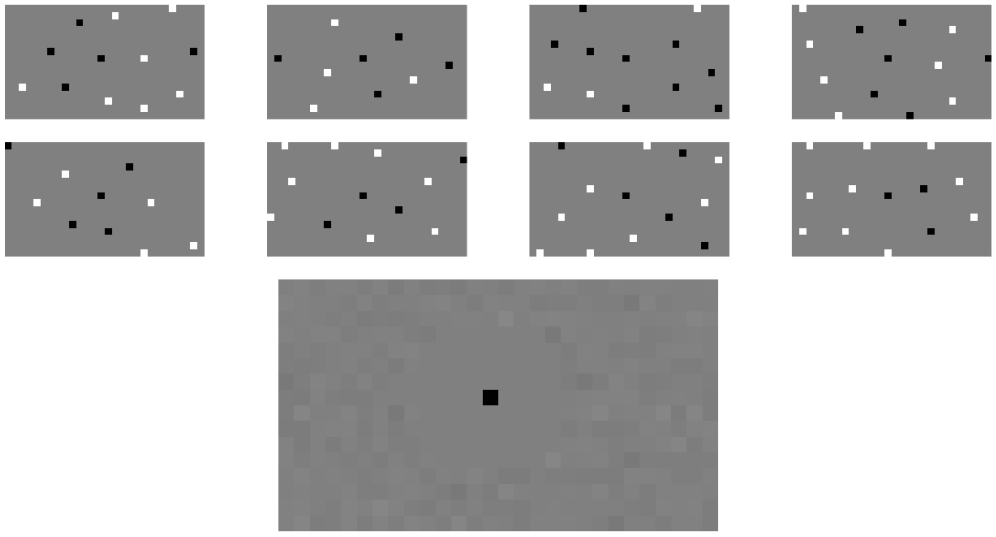

Figure 10. Locally sparse noise stimulus structure. A, Eight frames of the locally sparse noise stimulus when the central pixel was occupied by a black spot. **B,** The average of all of the frames when the central pixel was occupied by a black spot.

Each frame of the stimulus has ~11 spots (mean 11.4 ± 1.3 st dev) including both white and black. Each pixel was occupied by white and black pixels a variable number of times (mean 115 ± 11 (st. dev) for both white and black independently), and the mean intensity for each pixel was close to zero (mean 0.000013 ± 0.0016).

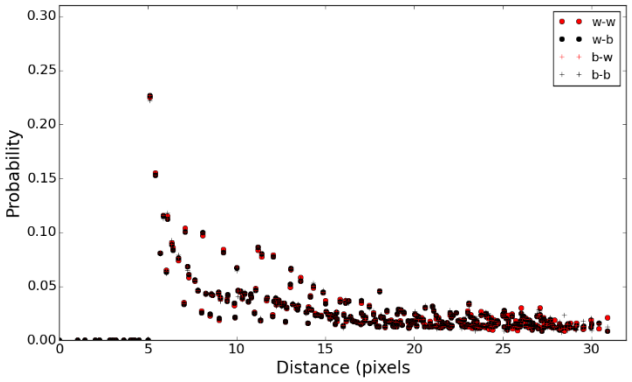

Figure 11. Probability of a pixel being occupied by a white (w) or black (b) square as a function of distance from the "central" pixel. The exclusion zone of 5 pixels is very clear. There is a higher probability of pixels just outside of the exclusion zone being occupied than further away. The probability of pixels being occupied, however, is the same regardless of the contrast of the central and outer pixel.

For data released in June 2017, the Session C stimulus was adapted to the Session C2 stimulus (**Fig. 4**). This stimulus session included 24 minutes of the Locally Sparse Noise 4 degree stimulus described above and 23 minutes of Locally Sparse Noise 8 degree stimulus. This second stimulus consisted of an 8 x 14 array made simply by scaling the 16 x 28 array used for the 4 degree stimulus. Please note, while the name of the stimulus is Locally Sparse Noise 8 degree, the actual pixel size is 9.3 degrees. The exclusions zone of 5 pixels was 46.5 degrees. This larger pixel size was found to be more effective at eliciting responses in the higher visual areas. Metrics and visualization for the higher visual areas (everything other than VISp) were computed using the "8

degree" stimulus, while the metrics and visualizations for VISp were computed using the "4 degree" stimulus. Responses to both stimuli are accessible in the NWB file and through the SDK.

> ***Important note:*** *The NWB files and SDK refer to these stimuli as Locally Sparse Noise 4 deg and Locally Sparse Noise 8 deg. The pixel sizes are in fact 4.65 and 9.3 degrees, respectively.*

Analysis. For each frame of the stimulus, the ΔF/F for each cell was calculated using the mean fluorescence of the preceding 1 second as the baseline F_0. As there is no inter-grating gray period, this 1 second window spans 4 different stimulus frames. The evoked response to each frame was defined as the mean change in fluorescence during the 0.5 second period following the start of the frame compared to the 1 second preceding the frame (**Fig. 11**). This 0.5 second response period spans both the presentation of the specified frame and the following frame.

The identification of responsive trials for each cell provides the starting point for all subsequent receptive field computational analysis. An automated algorithm is employed to categorize each trial in a binary fashion: a response is either detected or not. To accomplish this in an unsupervised fashion, two values are calculated on each trial: an approximation to the derivative in the ΔF/F signal is computed immediately after stimulus presentation, and again after a ~100 ms. delay. These two values are used to decouple the influence of calcium transients evoked during preceding trials, and the delay accounts for the transmission delay of signals through the early visual system. Using these values, a 2-dimensional Gaussian (noise) distribution near the origin can be fit to the samples across the entire experiment, after excluding outliers (**Fig. 12**). Any data point inside of a 4-sigma ellipse from this Gaussian are judged to be non-responsive trials; outliers from this ellipse (that are also positive and increasing in the delayed estimate of the derivative) are judged to be responsive trials. This results in trials judged to be responsive when there is an increasingly positive derivative in the ΔF/F across the trial interval, that is both delayed from stimulus onset and a statistically significant outlier from other trials in the same experiment.

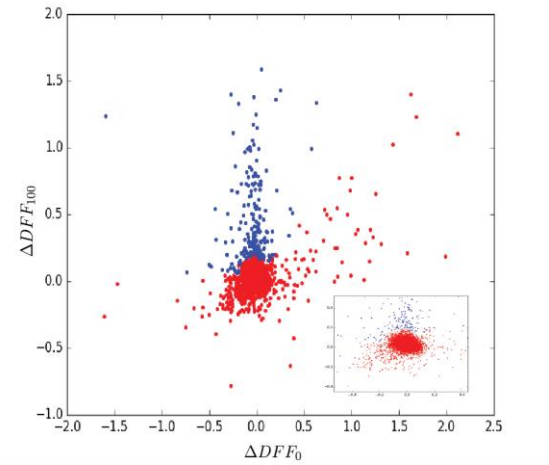

Figure 12. Isolating responsive from unresponsive trials. Two approximations to the derivative are computed for each trial, and scatter plotted. For each cell, a 2D Gaussian noise distribution is fit to the cluster near the origin. Outliers from this distribution with an increasing DF/F slope (i.e. positive ordinate and above identity line) are judged to be responsive trials. Inset: A zoomed view of the noise distribution near the origin.

The responsive trials were then used in two parallel analyses (**Fig. 13)**. First, chi-square tests were performed to identify cells that show non-uniform distributions of responses across pixels, a criterion for a receptive field. Given the structure of the locally sparse noise stimulus, described above, pixels cannot be present within 23 degrees of each other (or 46 degrees for the 9 degree pixels), thus the presence of a spatial receptive field in a region of visual space can be defined as a statistically-significant deviation from independence in the probability of responses across pixels. For each cell, a family of tests was performed across all pixel locations, performing a chi-square test that included both white and black pixels in a 7x7 grid, centered on the particular

pixel. Formally, each chi-square test asks whether the 98 pixels in the grid (i.e. black or white pixels in 7x7 locations = 98) have the same probability of evoking a response. A non-uniform distribution of response across neighboring pixels would indicate the presence of a receptive field. Performing this chi-square test across all pixel locations creates a map of p-values for each 7x7 grid. P-values were corrected for multiple comparisons performed across the entire monitor using the Šidák method. The output is a map of stimulus space where there is non-uniform distribution of responses and the location of the minimum p-value.

A second parallel analysis technique allows the identification of specific pixels in the visual stimulus that are correlated with responsive trials, separated into either responses to black or white stimulus pixels. Each stimulus pixel is convolved with a spatial Gaussian (4.65 degrees per sigma), to allow pooling of contributions to responses from nearby pixels. A p-value is computed for each pixel by constructing a null distribution for the number of trials in which a (black or white) pixel was present during responsive trials. This null distribution was estimated by shuffling the identity of the responsive trials (n=10,000 shuffles), breaking the relationship between stimulus and response under the assumption of a background level of responsiveness independent of the stimulus. In this way, statistical outliers (i.e. black or white pixels that were "on" when responses were detected more often that can be accounted for by chance) were identified by computing a p-value for each pixel relative to its null (shuffled) distribution. These p-values were corrected for false discoveries using the Šidák multiple comparisons correction, and thresholded at p=0.05 to identify pixel-wise statistically significant receptive field membership. The map of responsive trials is passed through these masks and fit with a 2-D Gaussian to parameterize the On and Off subunits.

For cells that have significant p-values for both analyses, the parameterized fits are included in database.

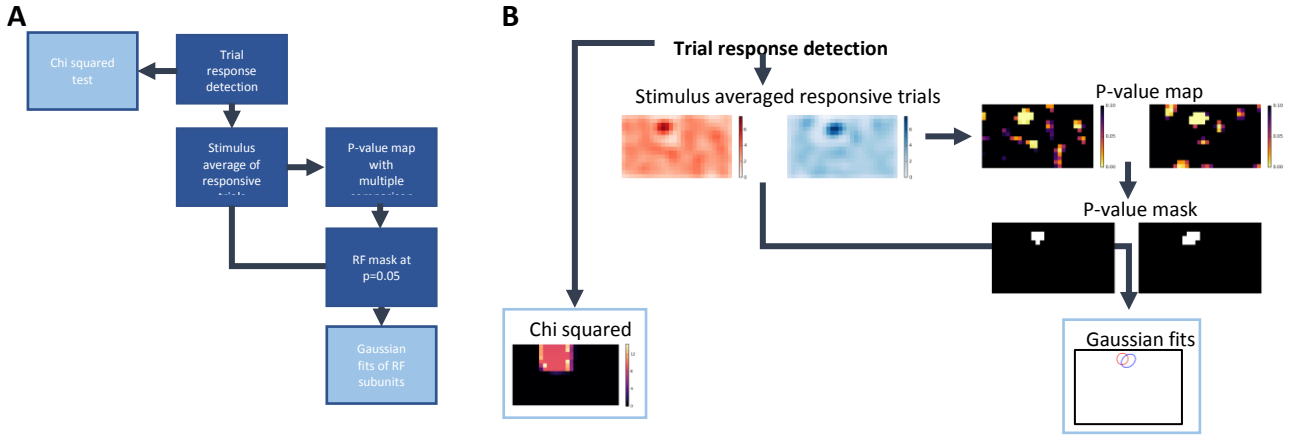

Figure 13. Receptive field analysis. A, Flow chart of receptive field analysis. Light blue boxes indicate the output that is included in the database for significant cells. **B,** Analyses intermediates for one example cell.

Visualization. The spatial receptive field for each cell is represented by two plots, showing the locations where the cell responded to white pixels (On) and black pixels (Off) (**Fig. 14**). For both On and Off, the mask of responsive pixels, created using the p-value map with multiple comparison correction, is applied to the stimulus average of responsive trials (see Fig. MM). The result is that only responsive pixels are shown, the strength of their response being indicated by the darkness of the color (red for On, blue for Off). This visualization captures the structure of On and Off subunits in the cell's spatial receptive field.

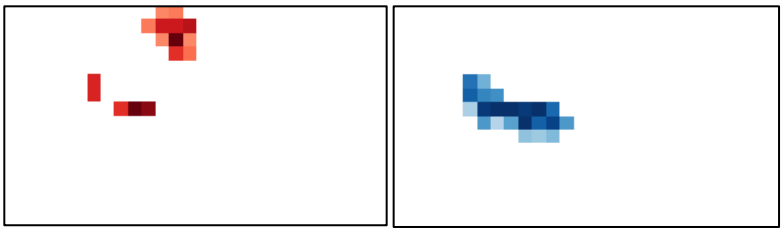

Figure 14. The receptive field heatmap represents responses to On (left) and Off (right) stimuli.

Due to the warping of the stimulus (see **Visual Stimulus Warping** description above), the outer most columns of the stimulus array fall off the monitor. The receptive field array that is accessible via the AllenSDK can be accessed with or without this mask.

The sum of all on and off subunits mapped in a given experiment is represented as the population receptive field (**Fig. 15)**. As nearby cells have receptive fields that cluster spatially, this population receptive field provides an estimate of what part of the visual field cells in an experiment are responsive to, even if each cell does not have a parameterized receptive field.

Figure 15. Population Receptive field

Natural Scenes

Stimulus. Receptive fields measured using synthetic stimuli, such as gratings and noise, often fail to predict responses to natural stimuli (David et al., 2004). This stimulus allows us to measure cells' responses to natural scenes to explore non-linear processing in their receptive fields.

The stimulus consisted of 118 natural images. Images 1-58 were from the Berkeley Segmentation Dataset (Martin et al., 2001), images 59-101 from the van Hateren Natural Image Dataset (van Hateren and van der Schaaf, 1998), and images 102-118 are from the McGill Calibrated Colour Image Database (Olmos and Kingdom, 2004). The images were presented in grayscale and were contrast normalized and resized to 1174 x 918 pixels. Images were luminance-matched, but a bug in our code resulted in an error in this matching such that the mean luminance of the images were not accurately matched, and were within 6% of each other.

The images were presented for 0.25 seconds each, with no inter-image gray period. Each image was presented ~50 times, in random order, and there were blank sweeps (i.e. mean luminance gray instead of an image) roughly once every 100 images.

Analysis. For each trial, the $\Delta F/F$ for each cell was calculated using the mean fluorescence of the preceding 1 second as the baseline F_o. As there is no inter-image gray period, this 1 second window spans 4 different image presentations. The evoked response to each image presentation was defined as the mean change in fluorescence during the 0.5 second period following the start of the image presentation compared to the 1 second preceding the image presentation (**Fig. 8**). This 0.5 second response period spans both the presentation of the specified image and the following image. Each image was presented ~50 times, and the responses to all presentations were averaged together. As the images were presented in random order, any effects of the

different images preceding or following the specified image should average out across the 50 trials. The preferred image was identified as the image that evoked the largest mean response.

*Metrics (see **Table 1**).* To determine if a cell was significantly responsive to the natural scene stimulus, a one-way ANOVA was computed comparing the responses to all of the 118 different images. A cell with a p-value less than 0.05 was considered to be responsive to this stimulus.

For the preferred image, the time-to-peak was measured as the time of the peak of the mean response relative to the onset of the image presentation.

The mean running speed of the mouse was computed for each image presentation. To calculate the running modulation, the presentations of the preferred image were broken into "stationary" trials (those when the speed was less than 1 cm/s) and "running" trials (those when the speed was greater than 1 cm/s). Provided that there were at least 10% of trials in each condition, the running modulation was defined:

$$run_{mod} = C \times \frac{R_{max} - R_{min}}{|R_{min}|}$$

where R_{max} is the larger of the response when the mouse is running or when the mouse is stationary, and R_{min} is the smaller of the two. If R_{max} is the response when the mouse is running, C=1. If R_{max} is the response when the mouse is stationary, C=-1.

The p_run value reports the p-value of an independent T-test comparing the mean responses of the stationary trials to the mean responses of the running trials.

To quantify how selective a cell is for images, the image selectivity was quantified using the following method (Quian Quiroga et al., 2007). The number of responses above a threshold, T, is computed as:

$$R(T) = \frac{1}{N}\sum_{i=1}^{N} \theta(f_i - T)$$

where f_i is the response of the neuron to image i, N is the number of images. *R(T)* is calculated for M=1000 threshold values, evenly spaced between the minimum and maximum responses:

$$T_j = f_{min} + j\frac{f_{max} - f_{min}}{M}$$

The area beneath the curve R(T) is calculated as:

$$A = \frac{1}{M}\sum_{j=1}^{M} R(T_j)$$

The image selectivity is

$$S = 1 - 2A$$

such that a uniformly responsive cell has a selectivity S=0, while a cell that responds to only one image has a selectivity S=1.

Visualization. Each cell's response to the natural scenes is captured by a "Corona plot," that captures the response to each image as well as the trial-to-trial variability of those responses (**Fig. 16A**). The responses to

all trials of a given image are represented by dots arranged as a ray extending from the center circle. The intensity of each dot corresponds to the cell's response to that trial, with the strongest response closest to the center and weaker responses radiating outward. The color scale of the dots ranges from white, which is the mean response to the blank sweep, to dark red, which is three standard deviations above the mean response to all stimulus conditions.

For each cell, we plot a histogram of the signal correlation of that cell with the other cells imaged in that experiment session, capturing the similarity of its tuning to the tuning of other cells. As the static gratings and natural scenes were presented in the same imaging session, the signal correlations of cells to these stimuli were plotted together, allowing comparisons of whether pairs of cells had similar correlations to these different stimuli (Fig. 9B).

The representational similarity matrix for each experiment is presented as a heatmap. Each row (and column) corresponds to a particular stimulus condition (e.g. a natural scene). The color of the element in the *i*th row and the *j*th column of the matrix indicates whether the mean response to stimulus *i* and *j* were positively correlated (red), negatively correlated (blue), or uncorrelated (white). The diagonal (*i=j*) was removed. (**Fig. 16B**).

We plot the comparison of signal and noise correlations for all cells in an experiment. As static gratings and natural scenes were presented in the same imaging session, these correlations are plotted in a single plot (**Fig. 9D**).

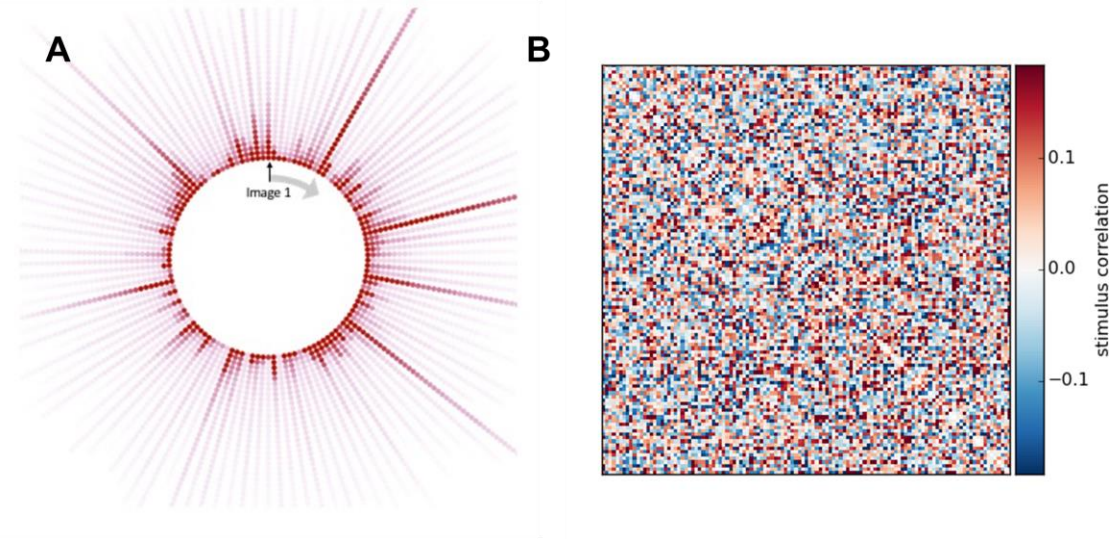

Figure 16. Visualizations of responses to natural scenes. A, The Corona Plot represents responses to natural scenes. **B,** Representational similarity matrix, here for responses to natural scenes. Histograms of signal correlation and the representational similarity matrix are shown in **Figure 9B.**

Natural Movies

Stimulus. This stimulus was used to measure responses to natural movies.

Three different clips were used from the opening scene of the movie *Touch of Evil* (Welles, 1958). This scene was chosen as it is a long take with a range of different features and scales of motion. Natural Movie 1 and Natural Movie 2 were both 30 second clips while Natural Movie 3 was a 120 second clip. All clips had been

contrast normalized and were presented in grayscale at 30 fps. Each movie was presented 10 times in a row with no inter-trial gray period.

Analysis. The response reliability was calculated as the mean trial-to-trial correlation:

$$reliability = \frac{2}{T^2 - T}\sum_{i=1}^{T}\sum_{j=i+1}^{T}\rho(f_i, f_j)$$

where f_i is the ΔF/F response of the i-th trial of a cell's preferred condition and T is the number of trials at the preferred condition (Rikhye and Sur, 2015).

Visualization. Each cell's response to the natural movies are represented by the "Track plot," capturing the response to each of the 10 presentations of the movie clip (**Fig. 17**). Each ring of the plot represents the cell's ΔF/F response to a single trial, represented as a heatmap binned in 1 second intervals. The movie begins at the top of the plot and proceeds clockwise around the circle. The inner rings, in red, show the responses to each of the 10 trials, while the outer blue ring represents the averaged response. The color scale ranges from white, which is ΔF/F=0, to dark red (or blue) which is three standard deviations above the mean response.

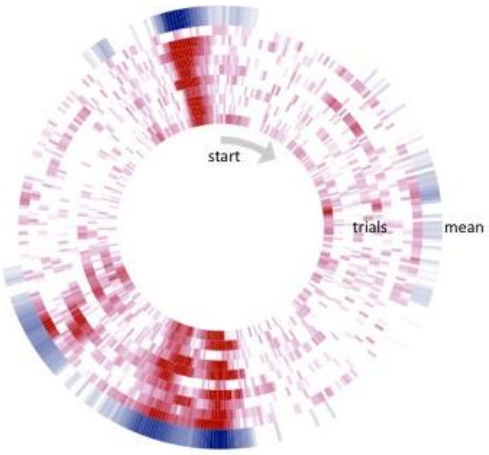

Figure 17. The track plot represents the responses to natural movies.

Spontaneous Activity

Stimulus. This stimulus was used to record activity from neurons when there is no structured visual stimulus being presented. The stimulus was 5 minutes of mean luminance gray.

Analysis. As of the June 2017 data release, no quantitative analysis of the spontaneous activity has been done.

Speed Tuning

Mice were positioned on a running disk during the imaging sessions, and a magnetic shaft encoder (US Digital) attached to this disk recorded the running speed of the mouse during the experiment at 60 samples per second. The running speed was down-sampled to match the timing of the 2-photon imaging (30 Hz).

Analysis. The tuning of cell activity to the mouse's running speed was quantified using a method similar to that found in Saleem et al. (Saleem et al., 2013). For each session the activity during the spontaneous activity

epoch(s) was analyzed independently from the rest of the session during which visual stimuli were present. The data was rank-sorted by the mouse's running speed, and discretized into a number of bins. The time points when the running speed was less than 1 cm/s were put into a single bin. All other time points were broken into equally sized bins containing 900 points. For each bin, the mean and standard error of the mean were calculated for both the running speed and the ΔF/F of each cell.

*Metrics (see **Table 1**).* The mean running speed of the mouse across each imaging session is calculated. This metric allows experiments with more or less running to be identified.

Visualization. Each cell's speed tuning is represented on a plot of the mean ΔF/F as a function of the mouse's running speed (**Fig. 18**), made by interpolating between the bins of running data described above. The stationary bin (speed <1 cm/s) is represented by a large dot. The speed tuning during visual stimuli is plotted in red, while the speed tuning during the spontaneous activity epoch(s) is shown in blue.

The running speed of the mouse for each experimental session is summarized with a histogram (**Fig. 19**).

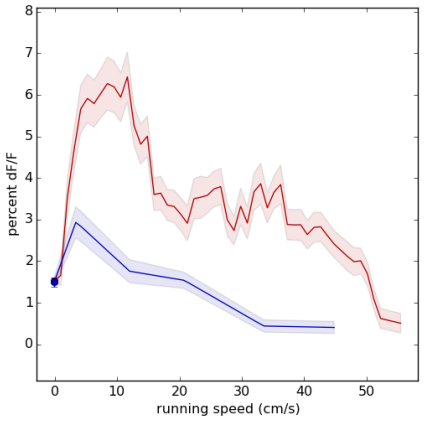

Figure 18. The speed tuning plot. The mean change in fluorescence (% ΔF/F) plotted as a function of running speed (cm/s).

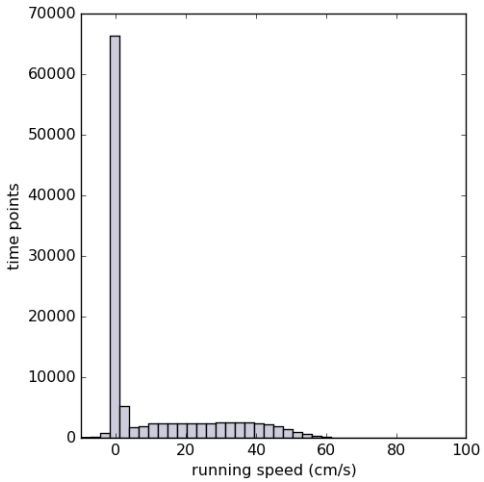

Figure 19. Running speed summary.

Table 1. Computed metrics

Metric	Stimulus	Description	Accessible from
Preferred direction	Drifting Gratings	Grating direction at the peak stimulus condition	Website, AllenSDK
Preferred temporal frequency	Drifting Gratings	Grating temporal frequency at the peak stimulus condition	Website, AllenSDK
Peak DFF	Drifting Gratings, Static Gratings, Natural Scenes	Mean response to peak stimulus condition	Website, AllenSDK
Orientation Selectivity Index	Drifting Gratings, Static Gratings	$OSI = \frac{R_{pref} - R_{orth}}{R_{pref} + R_{orth}}$	Website, AllenSDK
Global Orientation Selectivity Index	Drifting Gratings, Static Gratings	$gOSI = \frac{\sum R_\theta e^{2i\theta}}{\sum R_\theta}$	Website, AllenSDK
Direction Selectivity Index	Drifting Gratings	$DSI = \frac{R_{pref} - R_{null}}{R_{pref} + R_{null}}$	Website, AllenSDK
Global Direction Selectivity Index	Drifting Gratings	$gDSI = \frac{\sum R_\theta e^{i\theta}}{\sum R_\theta}$	Website, AllenSDK
Temporal frequency discrimination index	Drifting Gratings	$TFDI = \frac{R_{max} - R_{min}}{R_{max} - R_{min} + 2\sqrt{SSE/(N-M)}}$	Website, AllenSDK
P_value	Drifting Gratings, Static Gratings, Natural Scenes	One-way ANOVA comparing all stimulus conditions (including blank sweep).	Website, AllenSDK
Response reliability	Drifting Gratings, Static Gratings, Natural Scenes, Natural Movies	$reliability = \frac{2}{T^2 - T}\sum_{i=1}^{T}\sum_{j=i+1}^{T}\rho(f_i, f_j)$	Website, AllenSDK
Run modulation	Drifting Gratings, Static Gratings, Natural Scenes	$run_{mod} = C \times \frac{R_{max} - R_{min}}{\lvert R_{min}\rvert}$ If R_{max} is running condition, C=1. If R_{max} is stationary condition, C=-1. Only computed if at least 10% of trials in each condition.	Website, AllenSDK
Run p_value	Drifting Gratings, Static Gratings, Natural Scenes	Independent t-test of mean responses to peak stimulus condition when mouse is running (mean speed >1 cm/s) compared to mean responses to peak stimulus condition when mouse is stationary (<1 cm/s).	Website, AllenSDK
Preferred orientation	Static Gratings	Grating orientation at the peak stimulus condition	Website, AllenSDK
Preferred spatial frequency	Static Gratings	Grating spatial frequency at the peak stimulus condition	Website, AllenSDK

Metric	Stimulus	Description	Accessible from
Preferred phase	Static Gratings	Grating phase at the peak stimulus condition	Website, AllenSDK
Spatial frequency discrimination index	Static Gratings	$SFDI = \frac{R_{max} - R_{min}}{R_{max} - R_{min} + 2\sqrt{SSE/(N-M)}}$	Website, AllenSDK
Time-to-peak	Static Gratings, Natural Scenes	Time of the peak of the mean response to the peak stimulus condition, relative to the onset of the stimulus.	Website, AllenSDK
Preferred Image	Natural Scenes	Index of the image that elicits the peak response.	Website, AllenSDK
Image Selectivity	Natural Scenes	Metric of how selective a cell is for the images.	Website, AllendSDK
Chi-square p-value	Locally Sparse Noise	p-value of Chi square analysis	Website, AllenSDK
On Subunit Center X **On Subunit Center Y**	Locally Sparse Noise	Position (in x and y) of the centroid of the ON subunit	Website, AllenSDK
Off Subunit Center X **Off Subunit Center Y**	Locally Sparse Noise	Position (in x and y) of the centroid of the OFF subunit	Website, AllenSDK
Area ON	Locally Sparse Noise	Area of the ON subunit	Website, AllenSDK
Area OFF	Locally Sparse Noise	Area of the OFF subunit	Website, AllenSDK
Overlap	Locally Sparse Noise	Overlap Index of the ON and OFF subunits	Website, AllenSDK
Distance	Locally Sparse Noise	Distance between the centroid of the ON subunit and the OFF subunit	Website, AllenSDK

Metric Outlier Filtering. Some response metrics are not well defined under certain response conditions. This can lead to outlier metric values that should not be used for analysis. When this happens, we assign the metric a value of “NaN” (not a number). The criteria for NaN assignment are summarized in **Table 2**.

Table 2. Metric Outliers

Stimulus	Metrics	NaN Criteria	Reason
Drifting Gratings	osi_dg	p_dg >= 0.5 osi_dg < 0 osi_dg > 2	Insignificant response or negative DF/F (see comment below)
	dsi_dg	p_dg >= 0.5 dsi_dg < 0 dsi_dg > 2	Insignificant response or negative DF/F (see comment below)
	pref_dir_dg pref_tf_dg	p_dg >= 0.5	Insignificant responses cannot have a preferred stimulus condition

Stimulus	Metrics	NaN Criteria	Reason
Static Gratings	osi_sg	p_sg >= 0.5 osi_sg < 0 osi_sg > 2	Insignificant response or negative DF/F (see comment below)
	pref_ori_sg pref_sf_sg pref_phase_sg	p_sg >= 0.5	Insignificant responses cannot have a preferred stimulus condition
	time_to_peak_sg	p_sg >= 0.5 time_to_peak_sg < 0 time_to_peak_sg > 0.5	Peak response cannot begin prior to stimulus onset or after the next stimulus presentation
Natural Scenes	time_to_peak_ns	p_ns >= 0.5 time_to_peak_ns < 0 time_to_peak_ns > 0.5	Peak response cannot begin prior to stimulus onset or after the next stimulus presentation
	pref_image_ns	p_ns >= 0.5	Insignificant responses cannot have a preferred stimulus condition

REFERENCES

Andermann, M.L., Kerlin, A.M., Roumis, D.K., Glickfeld, L.L., and Reid, R.C. (2011). Functional specialization of mouse higher visual cortical areas. Neuron *72*, 1025–1039.

David, S., Vinje, W., and Gallant, J.L. (2004). Natural Stimulus Statistics Alter the Receptive Field Structure of V1 Neurons. J. Neurosci. *24*, 6991–7006.

DeAngelis, G.C., and Uka, T. (2003). Coding of Horizontal Disparity and Velocity by MT Neurons in the Alert Macaque. J. Neurophysiol. *89*, 1094–1111.

van Hateren, J.H., and van der Schaaf, a (1998). Independent component filters of natural images compared with simple cells in primary visual cortex. Proc. Biol. Sci. *265*, 359–366.

Hubel, D., and Wiesel, T. (1962). Receptive fields, binocular interaction and functional architecture in the cat's visual cortex. J. Physiol. *160*, 106–154.

Kriegeskorte, N., Mur, M., and Bandettini, P. (2008). Representational similarity analysis - connecting the branches of systems neuroscience. Front. Syst. Neurosci. *2*, 4.

Kuffler, S.W. (1953). Discharge patterns and functional organization of mammalian retina. J. Neurophysiol. *16*, 37–68.

Marshel, J.H., Garrett, M.E., Nauhaus, I., and Callaway, E.M. (2011). Functional specialization of seven mouse visual cortical areas. Neuron *72*, 1040–1054.

Martin, D., Fowlkes, C., Tal, D., and Malik, J. (2001). A database of human segmented natural images and its application to\nevaluating segmentation algorithms and measuring ecological statistics. Proc. Eighth IEEE Int. Conf. Comput. Vision. ICCV 2001 *2*, 416–423.

Olmos, A., and Kingdom, F.A.A. (2004). A biologically inspired algorithm for the recovery of shading and reflectance images. Perception *33*, 1463–1473.

Peirce, J.W. (2007). PsychoPy-Psychophysics software in Python. J. Neurosci. Methods *162*, 8–13.

Peirce, J.W. (2008). Generating Stimuli for Neuroscience Using PsychoPy. Front. Neuroinform. *2*, 10.

Quian Quiroga, R., Reddy, L., Koch, C., and Fried, I. (2007). Decoding Visual Inputs From Multiple Neurons in the Human Temporal Lobe. J. Neurophysiol. *98*, 1997–2007.

Rikhye, X.R. V, and Sur, M. (2015). Spatial Correlations in Natural Scenes Modulate Response Reliability in Mouse Visual Cortex. *35*, 14661–14680.

Ringach, D., Hawken, M.J., and Shapley, R. (1997). Dynamics of orientation tuning in macaque primary visual cortex. Nature *387*, 281–284.

Saleem, A., Ayaz, A., Jeffery, K., Harris, K., and Carandini, M. (2013). Integration of visual motion and locomotion in mouse visual cortex. Nat. Neurosci. *16*, 1864–1869.

Welles, O. (1958). Touch of Evil (United States: Universal - International).